Local field effects in half-metals: A GW study of zincblende CrAs, MnAs, and MnC

L. Damewood and C. Y. Fong

Phys. Rev. B **83**, 113102 — Published 22 March 2011

DOI: 10.1103/PhysRevB.83.113102

Local Field Effects in Half Metals—A GW Study of Zincblende CrAs, MnAs and MnC

L. Damewood and C. Y. Fong
Department of Physics, University of California Davis,
One Shields Avenue, Davis, California, 95616-8677, USA

We used the GW approximation to examine the improvements on the semiconducting gap in three predicted half metals with the zinc blende structure, CrAs, MnAs and MnC, compared to density functional theory with the generalized gradient approximation. Recognizing the differences between the local field effect in transition metals and insulators, respectively, we modeled one spin channel in a half metal as metallic having d-character and the oppositely oriented spin channel as insulating. In order to demonstrate the necessity of treating these three compounds as having d-character, we also applied the GW approximation to CrAs using the nearly free electron model in the conducting channel. We found that CrAs shows the least improvement while the Mn-based half metals exhibit comparable improvements. Physical explanations for these results are presented.

PACS numbers: 73.20.At,68.35.-p,75.50.Cc

Half metals, first predicted by de Groot *et al.*[1], are a promising class of materials for spintronic applications due to their inherently large (and integer unit Bohr magneton) magnetic moments ($\geq 1.0\,\mu_{\mathrm{B}}$) and complete spin polarization at the Fermi energy E_{F}. One spin channel of a half metal has a partially filled valence band, like a metal, while the oppositely oriented spin channel has a completely filled valence band, like an insulator or a semiconductor, resulting in 100% spin polarization at E_{F}. Types of half metallic compounds theoretically predicted so far include some Heusler alloys[2], such as Co_2FeSi, NiMnSb and PtMnSb[1]; some Si containing half Heusler alloys with Curie temperatures over 600 K[3], such as NiCrSi and PdCrSi; some transition-metal oxides, including rutile structured CrO_2[4,5]; some perovskites[6], such as $LaMnO_3$ and $SeMnO_3$; and a few more simply structured zincblende (ZB) compounds, including CrAs[7] and superlattices[8]. NiMnSb[9] and CrO_2[10] have been experimentally determined to be half metals at very low temperatures.

ZB CrAs was first predicted to be a half metal and then grown in thin film form by Akinaga *et al.*[7] It has many desirable properties that make it a good candidate for half metallic based spintronic devices: it has a simple stoichiometry, and is thus easier to control; it has a large magnetic moment of $3\,\mu_{\mathrm{B}}$; an experimentally estimated Curie temperature of over 400 K, well above room temperature; and it can be epitaxially grown as a thin film on a GaAs substrate[7]. Unfortunately, ZB half metals are meta-stable and do not exist in bulk form, since the ZB structure is not the ground state.

Despite their meta-stability, ZB half metals have inspired many theoretical studies. Pask *et al.*[11] studied CrAs, along with MnAs, MnC and other ZB materials, using pseudopotential and LAPW calculations with a generalized gradient approximation (GGA) exchange-correlation functional[12]. GGA and local density approximation (LDA) functionals are, however, known to underestimate the semiconducting gap. Additionally, devices containing half metals will have a biasing or gate voltage during operation so knowledge of the gap will determine an upper limit for the devices' operating voltages. In order to determine an accurate band gap in half metals, we turn to the so-called GW method[13], which is known to recover from the underestimated band gap of semiconductors and insulators[14]. In general, the improvement to the gap due to the GW method depends on the separation and the electronegativity difference between the ions[15].

The GW method is a many-body approach for electronic structure calculations that describes weakly interacting quasiparticles obeying the following equation:

$$h(x)\phi_i(x) + \int \mathrm{d}x'\, \Sigma(x,x')\phi_i(x') = \epsilon_i\phi_i(x), \tag{1}$$

where $h(x)$ is the single particle Hamiltonian; $\phi_i(x)$ and ϵ_i are the quasiparticle wavefunctions and energies, respectively; and $\Sigma(x,x')$ is the nonlocal, energy dependent self-energy which includes local field effects. Due to inhomogeneities in electron density on a scale smaller than the conventional unit cell, localized electric fields can polarize charges in insulators and semiconductors. These local fields are described by the off-diagonal ($\mathbf{G}-\mathbf{G}' \neq 0$) elements of the momentum $\mathbf{q}$, dependent dielectric matrix

$$\epsilon(\mathbf{q}+\mathbf{G},\mathbf{q}+\mathbf{G}'), \tag{2}$$

where $\mathbf{G}$ and $\mathbf{G}'$ are reciprocal lattice vectors. In metals, where the electron density does not vary substantially over short distances, the local field effect is small and the off-diagonal matrix elements of the dielectric matrix may be ignored[16].

The GW approach, in part by accurately accounting for local field effects and dynamical effects—such as the polarization of the electron gas due to a moving electron—has been extremely successful in improving the energy gap in semiconductors and insulators determined by LDA or GGA and agreeing to measurements of quasiparticle energies and lifetimes by direct or inverse photoemission experiments[14]. Within the GW approximation (GWA), complicated many-body vertex corrections are neglected and the self-energy is represented by the simple convolution $\Sigma = GW$ where G is the quasiparticle propagator and $W = \epsilon^{-1}V_{\text{coulomb}}$ is the screened Coulomb potential.

While half metals have properties of metals and insulators, approximations within the GW method have only been applied to systems that are either fully insulating or metallic. The conventional GW approach should be modified to treat the simultaneous existence of both types of electronic properties in half metals. In this paper, we investigate how the physical characteristics of the local fields in ZB half metals and the improvement of the semiconducting gap depend on the choice of transition metal and nonmetallic elements.

Due to the separate metallic and insulating spin channels, we treat the local field effect in each spin channel differently. In particular, the half metallic irreducible polarization $P(\text{Half metallic})$, is split between contributions from each spin channel:

$$\begin{aligned} P(\text{Half metallic}) &= \sum_{\sigma} P_{\sigma} \\ &= P_1(\text{Metallic}) + P_2(\text{Insulating}). \end{aligned} \tag{3}$$

The separation of the spin channels allows for the exclusion of local fields in the metallic channel while maintaining the treatment of local field effects in the other spin channel. Instead, if the material is an insulator, both spin channels are insulating and the fully insulating polarization would be

$$P(\text{Fully Insulating}) = P_1(\text{Insulating}) + P_2(\text{Insulating}). \tag{4}$$

The issue still remains whether the metallic channel in a ZB half metal should be treated in the nearly free electron model (simple metal), where only a single, $\mathbf{G} = 0$ vector is required[17], or as a transition metal, where localized d-electrons require the inclusion of many $\mathbf{G}$ vectors in the form of diagonal matrix elements[18].

By examining the charge density contributions near E_{F} in the metallic channel and near the top of the valence band in the insulating channel, we were able to justify the exclusion of the local fields in the metallic channel as well as determine if many or few $\mathbf{G}$ vectors are required to form the diagonal elements of the dielectric matrix. We used ZB CrAs as the prototypical example of the three ZB half metals. In Fig. 1, the density of states of the spin channels in CrAs are given with E_{F} set to zero. In Fig. 2(a), we show the charge density contribution in ZB CrAs to the metallic channel near E_{F} and in Fig. 2(b), we show the charge density contribution in the insulating channel at the top of the valence band E_{Top}, where the density of states is largest as seen in Figure 1(b). The levels of the contours in both charge distributions in Figure 2 are identical, so it is clearly seen that the distribution of charge in Fig. 2(a) is more homogeneous than the charge in Fig. 2(b). The uniformity of the charge density of the metallic channel as compared to the insulating channel demonstrates that the electrons in the majority spin channel are not expected to contribute substantially to the local fields. These considerable differences in the charge density justify the separate treatments of the local field effects in a ZB half metal. Furthermore, the distribution of charge in Fig. 2(a) still exhibits some d-character for these states near E_{F}. We are, therefore, not justified to treat the local field effect due to the metallic channel using the nearly free electron model, but instead, we must treat this spin channel like a transition metal.

Our approach accounts for all diagonal contributions ($\mathbf{G} = \mathbf{G}'$) to the dielectric matrix for the metallic channel and the full dielectric matrix for the insulating channel. This differs from the usual GW method in which the dielectric matrices for the two spin channels are treated either as both metallic or both insulating/semiconducting. For the purpose of comparison to the nearly free electron metal, we shall also calculate the GWA in CrAs, taking into account the extreme case of using only the $\mathbf{G} = \mathbf{G}' = 0$ contribution in the majority spin channel dielectric matrix, thereby treating the dielectric response as if the metallic channel has uniform charge density.

The software package ABINIT[19,20] was utilized to carry out the one-shot, spin-polarized, GWA using the Godby-Needs plasmon-pole model[21]. We initialized the GWA with a set of eigenfunctions and eigenenergies using the ionic pseudopotentials determined from the projector augmented wave (PAW)[22] scheme, with the GGA as the exchange correlation functional. In all three ZB half metals, we used planewave cutoff of 1600 eV and a (20,20,20) Monkhorst-Pack[23] $\mathbf{k}$-point mesh such that the total energy was converged to within 1 meV. The lattice constant of the CrAs unit cell, 5.66 Å, was determined by finding the lattice constant that minimizes the total energy within the initial PAW calculation while the lattice constants for MnAs (5.75 Å) and MnC (5.08 Å) were determined by finding lattice values that resulted in an integer magnetic moment. These results are in agreement with the previous study by Pask *et al.*[11] and Qian *et al.*[24] In addition, the exchange part of the self-energy matrix, Σ_{X}, was constructed using wavefunctions with a cutoff of 430 eV of kinetic energy and the corresponding self-energy matrix used 2685 $\mathbf{G}$ vectors.

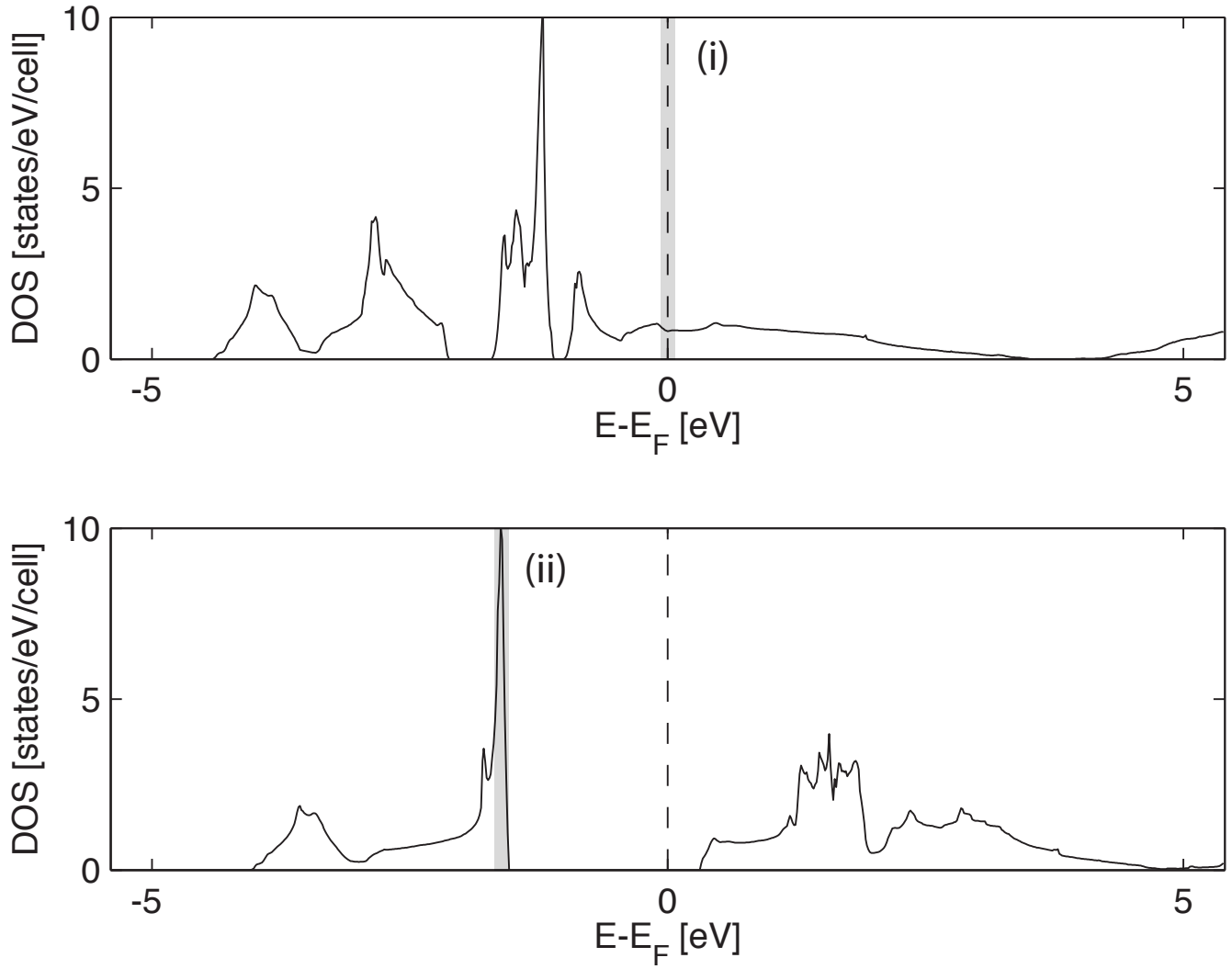

FIG. 1: Density of states of CrAs in (a) the majority spin channel and (b) the minority spin channel. Labels (i) and (ii) denote where the partial charge density in Figure 2 is taken from. Label (i) points to the 27.2 meV range around E_{F} in the metallic channel and label (ii) points to the small 27.2 meV range at the top of the insulating channel valence band.

We used the conventional GW approach, with a 181 $\mathbf{G}$ vector dielectric matrix for each spin channel, to handle the insulating case. In the half metallic case, we performed a similar calculation, but in accordance with our model, we excluded the off diagonal matrix elements of the metallic dielectric matrix only, representing the weak local field effect in that channel. To account for the extreme case of the nearly free electron model, an additional calculation was performed on CrAs that only included the $\mathbf{G} = \mathbf{G}' = 0$ term in the metallic-like channel.

Table I shows the values of the semiconducting gap using the PAW determined psuedopotentials with the GGA and three different treatments of the local field effect: fully insulating, transition metal and simple metal. The gap determined by the simple metal local field is presented for CrAs only. In general, the GGA exchange correlation functional is known to underestimate the gap by as much as 30%. In CrAs, the half metallic local field model widened the gap by 0.11 eV (6% increase) while the inclusion of the local field in the fully insulating local field model was different by only 0.04 eV (2%) demonstrating that the local fields in the metallic channel are indeed negligible. The first two GWA calculations on CrAs are in remarkable contrast to the half metallic local field model with only the single $\mathbf{G} = \mathbf{G}' = 0$ vector which widened the gap an additional 0.50 eV (23%). The widening of the gap in this case can be understood by the lack of participation of the metallic d-electrons in the short-ranged screening of the nuclear charges. When all but the long-ranged $\mathbf{G} = \mathbf{G}' = 0$ contributions are neglected, the localized d-electrons in the metallic channel cannot easily screen the nuclear charge. The resulting Coulomb potential W, causes the gap to increase by a significant amount. Since the metallic d-electrons should screen the nuclear charge, this last case is

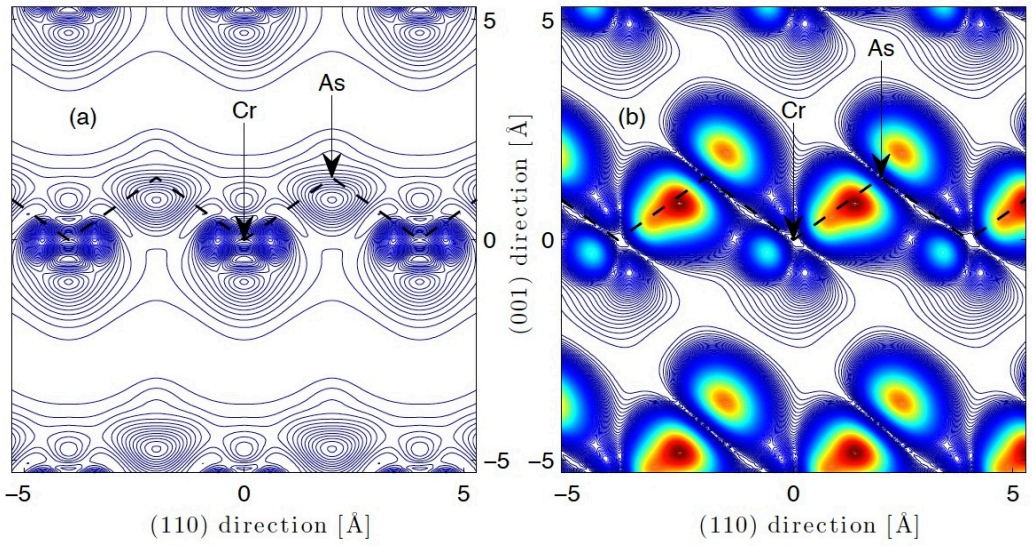

FIG. 2: (Color online) Charge density contributions in ZB CrAs (a) near E_F ($|E - E_F| \leq 13.6\,\text{meV}$) in the majority spin channel and (b) at the top of the valence band E_{Top} ($E_{\text{Top}} - 27.2\,\text{meV} \leq E \leq E_{\text{Top}}$), where the DOS is largest in the minority spin channel. Contour levels represent a difference of 0.02×10^{-5} electrons/cm^3 between lines. The majority spin channel (a) is relatively flat with a maximum charge density of 0.54×10^{-5} electrons/cm^3 compared to the minority spin channel (b) with a maximum charge density peak of 6.87×10^{-5} electrons/cm^3.

Half metal	Method	Gap [eV]
CrAs	PAW+GGA	1.85
	Fully insulating local field	1.92
	Half transition metal local field	1.96
	Half simple metal local field	2.46
MnAs	PAW+GGA	1.70
	Fully insulating local field	2.07
	Half transition metal local field	2.21
MnC	PAW+GGA	1.55
	Fully insulating local field	2.07
	Half transition metal local field	2.22

TABLE I: Semiconducting gaps in eV for ZB CrAs using four methods: the GGA as the exchange correlation functional, the fully insulating local field GWA, the half transition metal local field GWA using only $\mathbf{G} = \mathbf{G}'$ reciprocal lattice vectors in the metallic spin channel and the extreme case of the half simple metal local field GWA using a single $\mathbf{G} = 0$ reciprocal lattice vector in the metallic spin channel. The semiconducting gaps for MnAs and MnC are also provided within the first three methods.

physically unreasonable and shorter-ranged diagonal matrix elements should be included.

The influence of the extra d-electron in MnAs over CrAs explains both the greater increase in the GW gap over the GGA gap (0.52 eV in MnAs versus 0.11 eV in CrAs) and the 0.14 eV difference between the local field models. In MnAs, the extra d-electron produces a 4-fold increase in the peak electronic charge density near E_F in the metallic channel compared to CrAs illustrating the greater importance of the local fields. Likewise, MnC has a nearly identical electronic charge density peak in the metallic channel suggesting a similar local field effect. Additionally, MnC demonstrates how the electronegativity and the nearest neighbor distance affect the GW determined gap. The electronegativity of C (2.5) is twice as large as As[25] (1.25) and the lattice constant of MnC is much smaller than in MnAs resulting in a larger improvement over the GGA gap.

In summary, we have investigated the role of the local field effect in ZB half metals on the semiconducting gap using a modified GWA scheme based upon the physical circumstances in half metals. As electrons in the metallic channel are more delocalized than electrons in the insulating channel, the local field effect represented by the off-diagonal matrix elements in the dielectric matrix in the metallic channel may be ignored. However, due to the d-state character in the metallic channel of ZB half metals, the nonzero diagonal matrix elements ($\mathbf{G} = \mathbf{G}' \neq 0$) of the

dielectric matrix yield a significant contribution to the screening of nuclear charges. Among the three predicted half metals, MnAs and MnC both show a larger improvement over CrAs due to the extra electron in the transition metal element. The improvement in MnC is 0.15 eV larger than MnAs owing to the differences in the electronegativity of the non-metal elements and nearest neighbor separation distance. The improved, widened semiconducting gap will enable experimentalists to apply proper bias or gate voltages when the half metallic compounds are used for devices.

Acknowledgments

This research was supported in part by the National Science Foundation under grant number ECCS-0725902. This work was also supported by the National Science Foundation through TeraGrid resources provided by the National Center for Supercomputing Applications (NCSA).

[1] R. A. de Groot, F. M. Mueller, P. G. van Engen, and K. H. J. Buschow, Phys. Rev. Lett. **50**, 2024 (1983).
[2] F. Heusler, Verh. Dtsch. Phys. Ges. **5**, 219 (1903).
[3] V. A. Dinh, K. Sato, and H. Katayama-Yoshida, J. Supercond. Novel Magn. **23**, 79 (2010).
[4] K. Schwarz, J. Phys. F: Met. Phys. **16**, L211 (1986).
[5] K. P. Kämper, W. Schmitt, G. Güntherodt, R. J. Gambino, and R. Ruf, Phys. Rev. Lett. **59**, 2788 (1987).
[6] J. Park, E. Vescovo, H. Kim, C. Kwon, and R. Ramesh, Nature **392**, 794 (1998).
[7] H. Akinaga, T. Manago, and M. Shirai, Jpn. J. Appl. Phys., Part 2 **39**, L1118 (2000).
[8] C. Y. Fong, M. C. Qian, J. E. Pask, L. H. Yang, and S. Dag, Appl. Phys. Lett. **84**, 239 (2004).
[9] C. Hordequin, D. Ristoiu, L. Ranno, and J. Pierre, Eur. Phys. J. B **16**, 287 (2000).
[10] Y. Ji, G. J. Strijkers, F. Y. Yang, C. L. Chien, J. M. Byers, A. Anguelouch, G. Xiao, and A. Gupta, Phys. Rev. Lett. **86**, 5585 (2001).
[11] J. E. Pask, L. H. Yang, C. Y. Fong, W. E. Pickett, and S. Dag, Phys. Rev. B **67**, 224420 (2003).
[12] J. P. Perdew, K. Burke, and M. Ernzerhof, Phys. Rev. Lett. **77**, 3865 (1996).
[13] L. Hedin, Phys. Rev. **139**, A796 (1965).
[14] M. S. Hybertsen and S. G. Louie, Phys. Rev. B **34**, 5390 (1986).
[15] T. Lu and J. Zheng, Chemical Physics Letters **501**, 47 (2010).
[16] J. E. Northrup, M. S. Hybertsen, and S. G. Louie, Phys. Rev. Lett. **59**, 819 (1987).
[17] J. E. Northrup, M. S. Hybertsen, and S. G. Louie, Phys. Rev. B **39**, 8198 (1989).
[18] F. Aryasetiawan, Phys. Rev. B **46**, 13051 (1992).
[19] X. Gonze, J. Beuken, R. Caracas, F. Detraux, M. Fuchs, G.-M. Rignanese, L. Sindic, M. Verstraete, G. Zerah, and F. Jollet, Comput. Mater. Sci. **25**, 478 (2002).
[20] X. Gonze, G. Rignanese, M. Vertraete, J. Beuken, Y. Pouillon, R. Caracas, F. Jollet, M. Torrent, G. Zerah, M. Mikami, et al., Z. Kristall. **220**, 558 (2005).
[21] R. W. Godby and R. J. Needs, Phys. Rev. Lett. **62**, 1169 (1989).
[22] P. E. Blöchl, Phys. Rev. B **50**, 17953 (1994).
[23] H. J. Monkhorst and J. D. Pack, Phys. Rev. B **13**, 5188 (1976).
[24] M. C. Qian, C. Y. Fong, and L. H. Yang, Phys. Rev. B **70**, 052404 (2004).
[25] J. Phillips, *Covalent Bonding in Crystals, Molecules, and Polymers* (University of Chicago Press, Chicago, Il., 1969).